

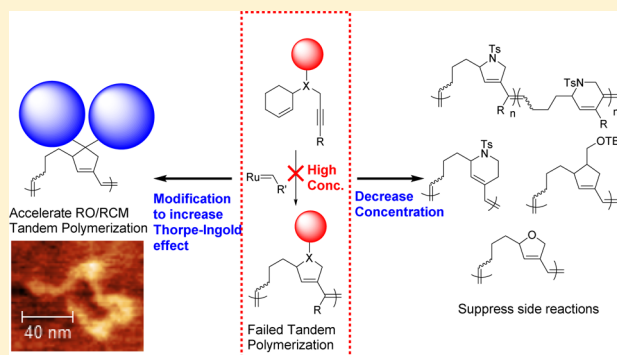
Versatile Tandem Ring-Opening/Ring-Closing Metathesis Polymerization: Strategies for Successful Polymerization of Challenging Monomers and Their Mechanistic Studies

Hyeon Park, Eun-Hye Kang, Laura Müller, and Tae-Lim Choi*

Department of Chemistry, Seoul National University, Seoul 151-747, Korea

S Supporting Information

ABSTRACT: Tandem ring-opening/ring-closing metathesis (RO/RCM) results in extremely fast living polymerization; however, according to previous reports, only monomers containing certain combinations of cycloalkenes, terminal alkynes, and nitrogen linkers successfully underwent tandem polymerization. After examining the polymerization pathways, we proposed that the relatively slow intramolecular cyclization might lead to competing side reactions such as intermolecular cross metathesis reactions to form inactive propagating species. Thus, we developed two strategies to enhance tandem polymerization efficiency. First, we modified monomer structures to accelerate tandem RO/RCM cyclization by enhancing the Thorpe–Ingold effect. This strategy increased the polymerization rate and suppressed the chain transfer reaction to achieve controlled polymerization, even for challenging syntheses of dendronized polymers. Alternatively, reducing the reaction concentration facilitated tandem polymerization, suggesting that the slow tandem RO/RCM cyclization step was the main reason for the previous failure. To broaden the monomer scope, we used monomers containing internal alkynes and observed that two different polymer units with different ring sizes were produced as a result of nonselective α -addition and β -addition on the internal alkynes. Thorough experiments with various monomers with internal alkynes suggested that steric and electronic effects of the alkyne substituents influenced alkyne addition selectivity and the polymerization reactivity. Further polymerization kinetics studies revealed that the rate-determining step of monomers containing certain internal alkynes was the six-membered cyclization step via β -addition, whereas that for other monomers was the conventional intermolecular propagation step, as observed in other chain-growth polymerizations. This conclusion agrees well with all those polymerization results and thus validates our strategies.



INTRODUCTION

The development of olefin metathesis reactions has provided a facile pathway to form carbon–carbon double bonds.¹ Over the past several decades, the efficiency of olefin metathesis has substantially increased with the development of well-defined catalysts based on ruthenium² and molybdenum.³ Organic chemists have developed ring-opening metathesis (ROM), ring-closing metathesis (RCM), and cross metathesis (CM) and have applied these reactions to various tandem metathesis reaction techniques to prepare complex organic molecules.⁴ Polymer chemists have applied these basic olefin metathesis reactions to various polymerizations such as ring-opening metathesis polymerization (ROMP),⁵ cyclopolymerization,⁶ and acyclic diene metathesis (ADMET)⁷ polymerization; these techniques have greatly expanded the synthetic tools available for polymer synthesis. However, most olefin metathesis polymerizations are still limited to these three basic metathesis reactions to give only simple polymer structures.^{6n,o,8}

To expand the versatility of olefin metathesis polymerization, tandem or cascade polymerization is highly desired; however,

because of poor selectivity among various functional groups, preparation of well-defined polymers has been challenging. Recently, we developed tandem ring-opening/ring-closing metathesis (RO/RCM) polymerization based on a selective cascade reaction between a terminal alkyne and a cycloalkene.⁹ Generally, polymerization of alkynes and cycloalkenes with low ring strain (e.g., cyclohexene) has been very challenging; ironically, however, when these two unreactive functional groups were fused into one monomer, a fast intramolecular RO/RCM reaction occurred even in living polymerization fashion. Furthermore, successful postmodification (e.g., Diels–Alder reaction on the polymer backbone) efficiently increased the polymer complexity. This method was also applied to prepare a sequence-controlled polymer.¹⁰ However, the monomer scope for this tandem polymerization was rather narrow because monomers containing nitrogen linker groups and terminal alkynes underwent efficient polymerization to give backbones containing pyrrolidines or piperidines, whereas

Received: November 23, 2015

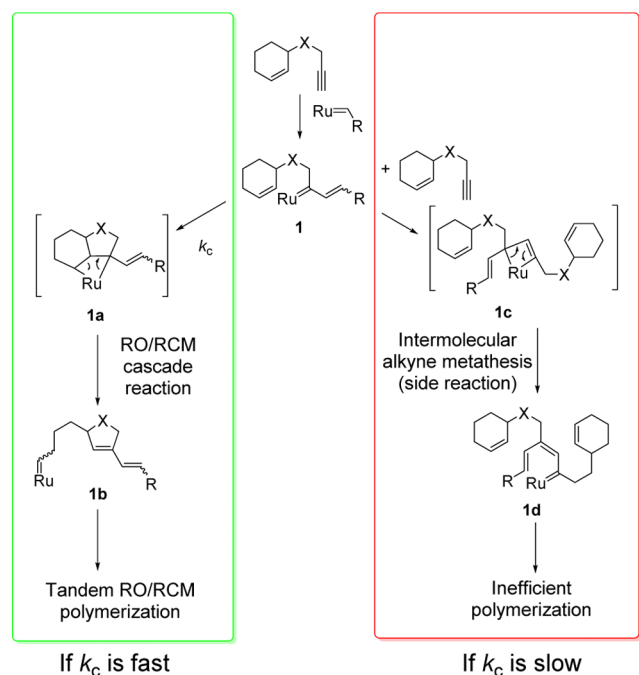
certain combinations of terminal alkynes and cycloalkenes did not undergo efficient polymerization.^{9b} We proposed in this previous work that instability of the highly fused multicyclic intermediate structures would lead to such failures.

We subsequently investigated the reaction profile in greater detail and speculated that a competing side reaction might shut down the tandem polymerization. This possibility led us to develop new polymerization strategies to increase the polymerization efficiency and expand the monomer scope. Herein, we report our successful attempts to greatly improve tandem RO/RCM polymerization and broaden the monomer scope to include challenging C and O linkers, internal alkynes, and even dendronized macromonomers. In this regard, two strategies—modifying the monomers to enhance the Thorpe–Ingold effect¹¹ and lowering the reaction concentration—successfully directed the reaction pathways toward effective polymerization rather than toward side reactions. Detailed kinetic analysis provided deep insights into the mechanism to explain the interesting polymerization behaviors and to validate our logic.

RESULTS AND DISCUSSION

Previously, we successfully demonstrated tandem RO/RCM polymerization of monomers containing nitrogen linker groups, cycloalkenes, and propargyl groups. These optimized monomers exhibited extremely fast polymerization, with full conversion within 1 min at room temperature or 10 min at $-30\text{ }^{\circ}\text{C}$.⁹ However, when monomers containing an analogous homopropargyl group or carbon or oxygen linker group underwent polymerization, their efficiencies were very low or they were totally inactive.^{9b} In this previous work, we proposed that the polymerization reactivity was governed by monomer structures that might affect the stability of metalcyclobutane intermediates (such as **1a** in Scheme 1) during tandem RO/RCM reactions. We then sought other possible reasons for the low reactivity. During tandem polymerization, the initiator

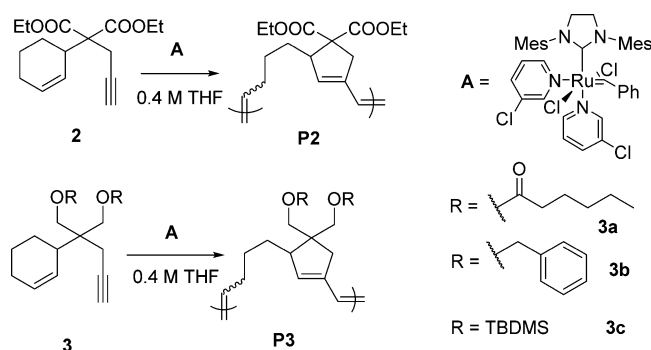
Scheme 1. Possible Competing Reaction during the Tandem RO/RCM Process



reacted with an alkyne in α -addition manner to form a 1,1-disubstituted metal carbene intermediate (**1**); the resulting intermediate underwent an intramolecular tandem RO/RCM reaction (**1a**) to form a propagating species (**1b**).⁹ However, if this intramolecular cyclization rate (k_c) was relatively slow, metal carbene intermediate **1** would undergo side reactions such as intermolecular CM (**1c**), which would then afford inactive propagating species (**1d**). On the basis of this proposal, we devised two strategies to favor cyclization selectivity, thereby enhancing the tandem polymerization reaction pathway.

We first focused on designing new monomers to accelerate the intramolecular RO/RCM reaction by enhancing the Thorpe–Ingold effect. In our previous work, unsuccessful polymerization of a monomer containing a carbon linker might have been due to a small monosubstituted ester side chain.^{9b} To improve polymerization, we added an additional ester substituent to the monomer to enhance the Thorpe–Ingold effect; as a result, disubstituted monomer **2** underwent successful tandem polymerization in the presence of a third-generation Grubbs catalyst (**A**)¹² to yield a high-molecular-weight polymer, with 80% monomer conversion after 90 min at room temperature (Table 1, entry 1).^{6fj,m} Although this

Table 1. Polymerization of Monomer with Disubstituted Carbon Linker



entry	monomer (M/I)	time	temp	conv ^a	M_n /PDI ^b
1	2 (50)	90 min	rt	80%	20 k/1.49
2	3a (50)	20 min	rt	100%	33 k/1.99
3	3a (50)	15 min	$-10\text{ }^{\circ}\text{C}$	100%	26 k/1.17
4	3a (100)	30 min	$-10\text{ }^{\circ}\text{C}$	87%	48 k/1.79
5	3b (50)	1 min	rt	96%	16 k/1.18
6	3b (75)	1.5 min	rt	100%	26 k/1.11
7	3b (100)	2 min	rt	100%	33 k/1.32
8	3b (150)	3 min	rt	80%	37 k/1.35
9	3c (50)	30 s	rt	100%	27 k/1.25
10	3c (100)	30 s	rt	95%	50 k/1.37
11	3c (75)	8 min	$0\text{ }^{\circ}\text{C}$	100%	34 k/1.14
12	3c (100)	10 min	$0\text{ }^{\circ}\text{C}$	100%	50 k/1.27
13	3c (150)	20 min	$0\text{ }^{\circ}\text{C}$	100%	84 k/1.44

^aConversion determined by crude ^1H NMR. ^bDetermined by THF SEC, calibrated using polystyrene (PS) standards.

strategy appeared to be successful, polymerization of **2** was still slow when compared to polymerization of the previously reported sulfonamide monomers that exhibited complete conversion within 1 min under the same reaction conditions.⁹ We reasoned that the relatively low reactivity of monomer **2** was due to the small size of the ester substituent (A -value of $-\text{COOR}$: 1.27 kcal/mol)¹³ and that changing the substituents

to larger methoxy derivatives would increase the polymerization reactivity (A -value of $-\text{CH}_2\text{OH}$: 1.8 kcal/mol).¹³

Tandem polymerization of monomer **3a** with hexanoyl groups underwent complete conversion within 20 min at room temperature to give a high-molecular-weight polymer; however, the polydispersity index (PDI) of this polymer was disappointingly broad because of the chain transfer reaction (entry 2).⁹ The chain transfer reaction was suppressed when the reaction temperature was reduced to $-10\text{ }^\circ\text{C}$ (entry 3), but the PDI was still broad for polymerization at a higher monomer-to-initiator (M/I) ratio (entry 4). To achieve living polymerization, monomers containing even larger substituents are necessary to enhance polymerization reactivity and suppress the chain transfer reaction. Thus, monomer **3b** containing bulkier benzyl ether substituents was synthesized, and the polymerization of **3b** yielded 96% monomer conversion within 1 min; in addition, the PDI was narrower than 1.2 (entry 5). The molecular weights of **P3b** were linearly controlled by increasing the M/I ratio such that the degree of polymerization (DP) was 120 and the PDIs remained relatively narrow (entries 5–8, Figure 1). A monomer with bulkier *tert*-butyldimethylsilyl

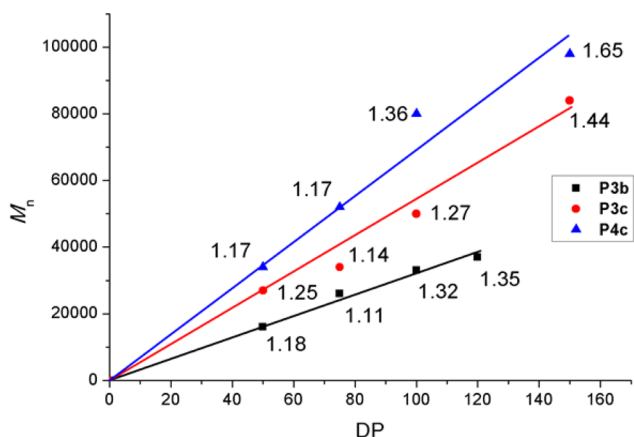
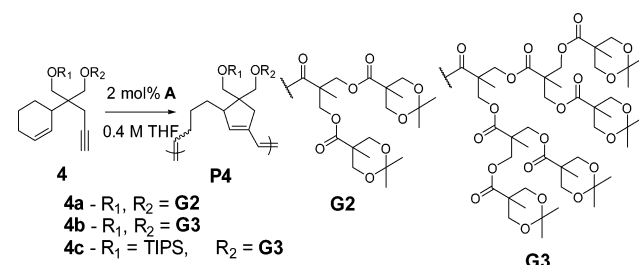


Figure 1. Plot of M_n versus DP for **P3b**, **P3c**, and **P4c**. The PDI values are shown as labels.

(TBDMS) substituents (**3c**) exhibited even higher reactivity, with complete monomer conversion within 30 s to give **P3c** with a narrow PDI (entry 9). This monomer appeared to be more reactive than the previously reported amide analogues.⁹ To ensure controlled polymerization, we decreased the reaction temperature to $0\text{ }^\circ\text{C}$ to give **P3c** with a narrower PDI; the molecular weight was well controlled to a DP of 150 (entries 10–13, Figure 1). These data suggested that the modification of monomer structures to enhance the Thorpe–Ingold effect was indeed a successful strategy to increase tandem polymerization reactivity and to achieve living polymerization.

To demonstrate the effectiveness of this strategy, we attempted tandem polymerization of even more challenging monomers to synthesize dendronized polymers via a macromonomer approach.^{6f,14} Although the macromonomer approach to dendronized polymers was extremely challenging because of the highly bulky dendron substituents, these dendrons could also induce a strong Thorpe–Ingold effect to increase polymerization reactivity. Initially, **4a** containing bis-substituted second-generation ester dendrons (**G2**)¹⁵ was tested and resulted in complete conversion to a polymer after 2 h ($M/I = 50$) (Table 2, entry 1). However, monomer **4b** containing two larger third-generation dendrons (**G3**) did not

Table 2. Polymerization of Monomer with Dendronized Substituent



entry	monomer (M/I)	time	temp.	conv ^a	M_n /PDI ^b
1	4a (50)	2 h	rt	100%	33 k/1.39
2	4b (50)	8 h	rt	0%	—
3	4c (50)	1 h	rt	100%	34 k/1.17
4	4c (50)	1.75 h	rt	100%	52 k/1.17
5	4c (100)	2.5 h	rt	100%	80 k/1.36
6	4c (150)	3.5 h	rt	100%	98 k/1.65

^aConversion determined by crude ^1H NMR. ^bDetermined by THF SEC, calibrated using polystyrene (PS) standards.

polymerize at all after long reaction times (entry 2). The excessively bulky **G3** bis-substituents likely blocked the catalyst approach to the alkyne. To solve this problem, we substituted one of the **G3** bis-substituents to a smaller triisopropylsilyl (TIPS) substituent; as a result, monomer **4c** was completely converted into a 50-mer dendronized polymer with a narrow PDI within 1 h (entry 3). Furthermore, the controlled polymerization of **4c** was successful for M/I ratios up to 150 (entries 3–6, Figure 1).

A substantial advantage of the dendronized polymer having bulky side chains was that it allowed us to clearly observe a single chain of the polymer by atomic force microscopy (AFM). Indeed, Figure 2 shows the relatively stretched chains of **P4c**

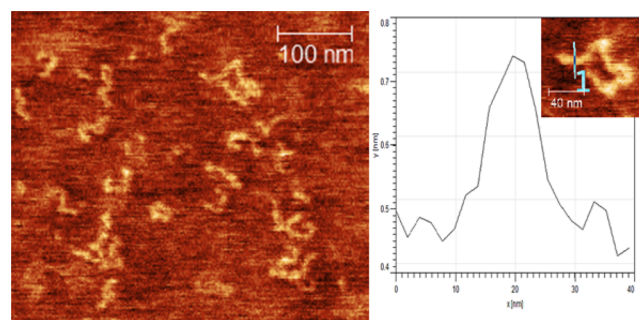


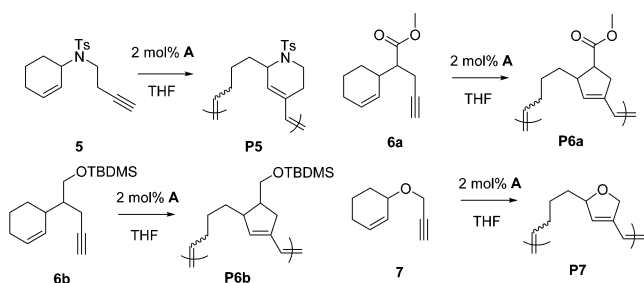
Figure 2. AFM image of **P4c** in phase mode and single-chain height profile in height mode. The polymer solution in DCM (1.25 mg/L) was spin-coated onto a mica surface.

for the 100-mer polymer whose length and height were approximately 75 and 0.3 nm, respectively. The rigidity of **P4c** was similar to that of polynorbornene-based dendronized polymers^{14a} but was certainly less than that of polymers prepared by cyclopolymerization^{6f,m} or ROMP of *endo*-tricyclo[4.2.2.0]deca-3,9-diene^{14b} with the same dendron structure and dendron generation. This was due to the presence of a flexible methylene polymer backbone, which increased the conformational freedom of the polymer chain.

Although modifying monomer structures was an effective strategy to increase polymerization reactivity, an alternate strategy was required in cases where the monomer structures

could not be modified. In such cases, we applied the second strategy of suppressing intermolecular side reactions by reducing the monomer concentration (Scheme 1). Previously, we reported that monomers containing a homopropargyl group (5), monosubstituted carbon (6a and 6b), or oxygen linker (7) did not yield polymers at the 0.4 M concentration, which is the concentration typically used for this tandem polymerization (Table 3, entries 1–4).^{9b} However, when the monomer

Table 3. Polymerization of Monomers with Low Reactivity



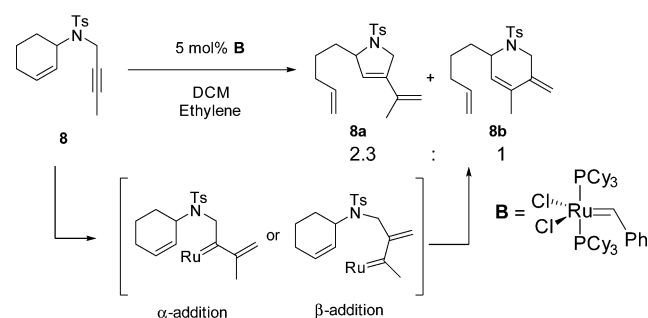
entry	mono	concn	time/temp	conv ^a	M _n /PDI ^b
1	5	0.4 M	12 h/rt	10%	—
2	6a	0.4 M	12 h/rt	0%	—
3	6b	0.4 M	12 h/rt	16%	—
4	7	0.4 M	12 h/rt	0%	—
5	5	0.03 M	3 h/40 °C	100%	26 k/1.50
6	6a	0.01 M	6 h/rt	95%	6.2 k/1.34
7	6b	0.03 M	3 h/rt	100%	7.7 k/2.88
8	7	0.03 M	30 min/rt	100%	3.6 k/1.51

^aConversion determined by crude ¹H NMR. ^bDetermined by THF SEC calibrated using polystyrene (PS) standards.

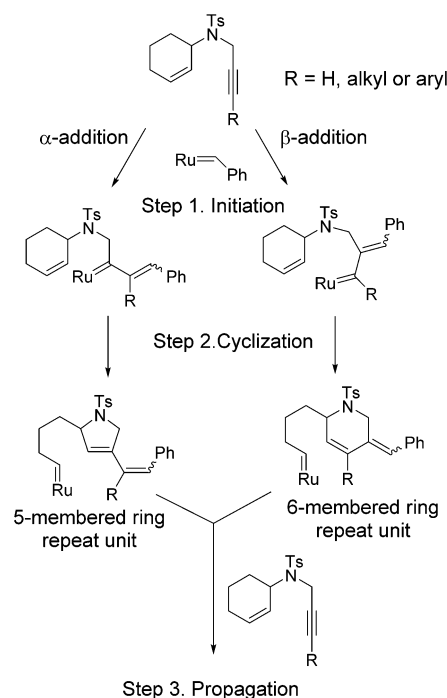
concentration was decreased from 0.4 to 0.03 or 0.01 M (for 6a containing a smaller substituent, conversion at 0.03 M was only 53% presumably due to even slower cyclization), all four monomers underwent excellent conversion at room temperature or at slightly elevated temperature (40 °C for 5) (entries 5–8). These results indicate that the intramolecular RO/RCM reaction was indeed slow for these monomers (Scheme 1) and that consequently the competing side reaction stopped the tandem polymerization. Gratifyingly, simple dilution solved this problem. However, the polymerization reactions at low concentrations were inevitably much slower and the PDIs also broadened (Table 3).

With these successful strategies to promote efficient polymerization of various monomers, we focused on an even broader monomer scope by using monomers with internal alkynes instead of terminal alkynes. Polymerization of the internal alkynes was even more challenging because of steric hindrance from the additional substituent. Moreover, unlike terminal alkynes, which exclusively undergo α -addition,^{6,9} internal alkynes undergo both α -addition and β -addition nonselectively, thereby forming complex polymer microstructures.¹⁶ As a control experiment, we tested the ring rearrangement reaction of 8 by performing ethenolysis with a first-generation Grubbs catalyst (B) and obtained two different products, 8a and 8b, in a 2.3:1 ratio (Scheme 2; see Supporting Information (SI) for details). This result suggested that tandem polymerization of monomers containing internal alkynes would also form both five- and six-membered-ring repeating units as a result of nonselective α - and β -addition (Scheme 3).

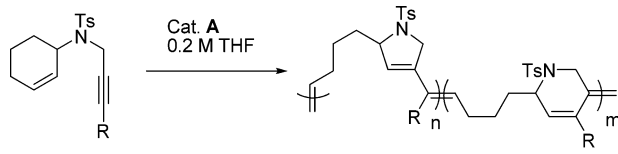
Scheme 2. Ring Rearrangement of a Monomer Containing Internal Alkyne 8 by Ethylene



Scheme 3. Possible Reaction Mechanism of a Monomer with Internal Alkyne



Initially, we attempted the tandem polymerization of monomer 8 at a concentration of 0.4 M, but it only yielded 50% monomer conversion after 2 h, with a broad PDI (Table 4, entry 1). We subsequently used the dilution strategy and observed that reducing the concentration to 0.2 M increased the conversion to 93% within just 5 min. Notably, this polymerization occurred rapidly and the resulting PDI was 1.2 (entry 2). ¹H NMR analysis of P8 showed two different sets of signals corresponding to five- and six-membered-ring repeating units with an identical ratio of 2.3:1, favoring α -addition (Scheme 2). When the reaction temperature was lowered to 15 °C, the chain-transfer reaction was further suppressed and the PDI became narrower than 1.1 (entry 3). Again, we observed well-controlled polymerization behavior, where the molecular weight and DP exhibited a linear relationship up to a DP of 190 and the PDIs were narrow (entries 3–6, Figure 3). Similarly, controlled polymerization of monomer 9, which contained an ethyl-substituted alkyne, was successful at 10 °C (entries 7–10, Figure 3). A slight increase in steric bulkiness provided by an ethyl substituent (*A*-value: 1.75 kcal/mol)¹³ in place of the methyl substituent (*A*-value: 1.70 kcal/mol)¹³ decreased the

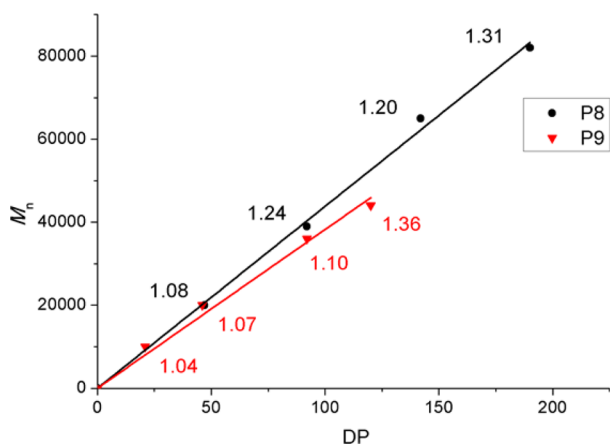
Table 4. Tandem Polymerization of Monomers Containing an Internal Alkyne


8 - R = Me
9 - R = Et
10 - R = CF₃

P8 - R = Me
P9 - R = Et
P10 - R = CF₃

entry	mono (M/I)	time/temp	conv ^a	M _n /PDI ^b	n:m ^c
1 ^c	8 (50)	2 h/rt	50%	15 k/1.50	2.3:1
2	8 (50)	5 min/rt	93%	30 k/1.20	2.3:1
3	8 (50)	10 min/15 °C	93%	20 k/1.08	2.3:1
4	8 (100)	14 min/15 °C	92%	39 k/1.24	2.3:1
5	8 (150)	15 min/15 °C	95%	65 k/1.20	2.3:1
6	8 (200)	20 min/15 °C	95%	82 k/1.31	2.3:1
7	9 (25)	5 min/10 °C	85%	10 k/1.04	1.7:1
8	9 (50)	25 min/10 °C	92%	20 k/1.07	1.7:1
9	9 (100)	30 min/10 °C	92%	36 k/1.10	1.7:1
10	9 (150)	40 min/10 °C	80%	44 k/1.36	1.7:1
11	10 (50)	10 min/rt	100%	16 k/1.06	1:0
12	10 (100)	1.5 h/15 °C	89%	42 k/1.15	1:0
13	10 (150)	2.5 h/15 °C	80%	49 k/1.44	1:0

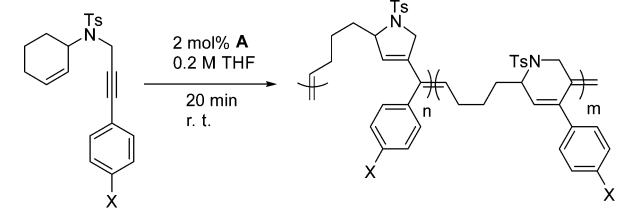
^aDetermined by crude ¹H NMR. ^bDetermined by THF SEC calibrated using polystyrene (PS) standards. ^cReaction concentration was 0.4 M.

**Figure 3.** Plot of M_n versus DP for P8 and P9. Numbers on the line indicate PDIs.

selectivity between α -addition and β -addition to give a 1.7:1 ratio (see Supporting Information for details).

Lastly, we studied the polymerization of monomer **10**, which contained an electron-withdrawing trifluoromethyl (CF₃) substituent. For an M/I ratio of 50, monomer **10** was completely converted to a polymer with a PDI narrower than 1.1 (entry 11). For high M/I ratios, a decrease in the reaction temperature to 15 °C appeared to result in greater polymerization efficiency (entries 12 and 13). Interestingly, although the *A*-value of the CF₃ substituent is greater than that of a methyl or ethyl substituent (*A*-value: 2.1 kcal/mol),¹³ only a five-membered-ring polymer unit was observed for P10, implying that α -addition occurred exclusively (see Supporting Information for details). These results suggested that the regioselectivity was dependent on not only the steric bulk but also the electronic effects of the alkyne substituent.

To investigate the electronic effects of the substituent toward the polymerization, we investigated the structure–reactivity relationship of monomers containing internal alkyne substituents with the same steric effect but different electronic effects. Therefore, we prepared several monomers containing 4-substituted phenyl substituents (**11a–e**) and tested for tandem polymerization with 2 mol % of catalyst **A** for 20 min. Monomer **11c**, which contained a neutral phenyl substituent, exhibited 73% conversion, whereas monomers with electron-donating groups (**11a**, **11b**) showed less than 40% conversion (Table 5, entries 1–3) and monomers with electron-with-

Table 5. Polymerization of Monomer with Phenyl Derivatives


11a - X = OMe
11b - X = Me
11c - X = H
11d - X = F
11e - X = CF₃

P11a - X = OMe
P11b - X = Me
P11c - X = H
P11d - X = F
P11e - X = CF₃

entry	monomer	conv ^a	M _n ^b	PDI ^b	n:m ^c
1	11a	22%	—	—	—
2 ^d	11b	33%	27 k	1.31	—
3	11c	73%	22 k	1.25	2:1
4	11d	85%	34 k	1.31	2.7:1
5	11e	85%	30 k	1.48	1:1

^aConversion determined by crude ¹H NMR. ^bDetermined by THF SEC calibrated using polystyrene (PS) standards. ^cRatio determined by ¹³C NMR. ^dSEC measurement was performed with crude polymerization sample because purification of polymer failed.

drawing groups (**11d**, **11e**) showed 85% conversion (entries 4 and 5). Although the steric effects of phenyl substituents are quite high (*A*-value: 3.00 kcal/mol),¹³ the ratio between five- and six-membered-ring units varied from 1:1 to 2.7:1 for P11c–e, as determined by ¹³C NMR experiments (see Supporting Information for details). This complex α - and β -addition selectivity appears to originate from the electronic effects of phenyl substituents.

To further elucidate the electronic effects of various phenyl substituents, we measured the early stage of the polymerization kinetics (initial rates) and constructed Hammett plots (Figures 4a and 4b) from the propagation rate constants (see Supporting Information for experimental details). The plots showed positive linear relationships between the Hammett constant (σ_p) and $\log(k_X/k_H)$ ($\rho = 0.44$), indicating that the polymerization rate was accelerated by electron-withdrawing groups on the phenyl substituent. Similar ρ values were reported by Chen et al., who investigated the structure–reactivity relationship in olefin metathesis reactions involving benzylidenes with various electronic effects.¹⁷ They explained that electron-deficient ruthenium benzylidenes reacted faster than electron-rich benzylidenes because electron-deficient benzylidenes were destabilized to a greater extent. For the tandem RO/RCM polymerization, β -addition of propagating carbene to alkynes formed a benzylidene intermediate (not an

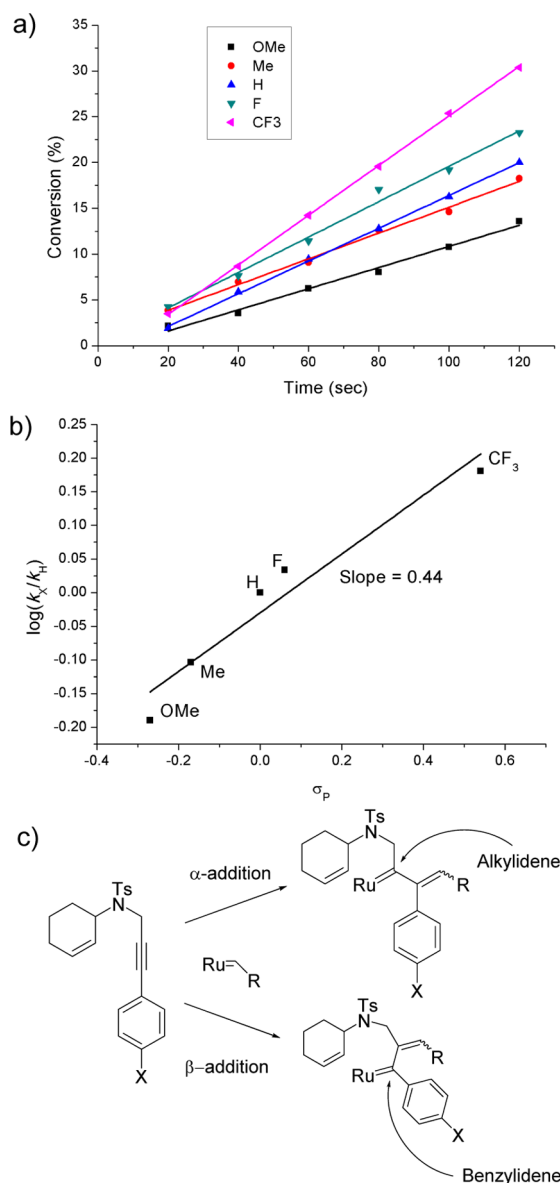


Figure 4. (a) Plot of the polymerization rate of phenyl derivative monomers. (b) Hammett plot of phenyl derivative monomers. (c) Possible intermediates from the alkyne initiation step.

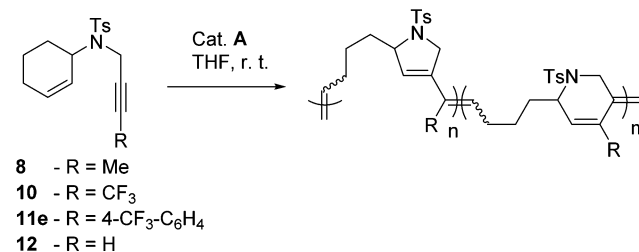
alkylidene intermediate formed after α -addition), whose reactivity was directly governed by the electronic effects of phenyl substituents, similar to the results reported by Chen et al. (Figure 4c).¹⁷ On the basis of the kinetics data, we concluded that the rate-determining step involves intermediates that would show the electronic effect on phenyl substituents to affect the polymerization rate.

A detailed understanding of the mechanism would require determination of the rate-determining step of tandem polymerization through a series of kinetics studies. Tandem RO/RCM polymerization fundamentally consists of two steps: the intermolecular propagation step between a growing active alkylidene and other monomers, followed by the intramolecular RO/RCM cyclization step forming the ring structure. Polymerization kinetics became more complex for monomers containing internal alkynes because, depending on the selectivity of α - or β -addition, two different intermediates could form and undergo five- or six-membered-ring cyclization

with different reaction rates (Schemes 1 and 3). With these polymerization pathways in mind, we performed kinetics studies by measuring the initial rates for tandem RO/RCM polymerization at monomer concentrations ranging from 0.01 to 0.03 M to exclude any possible side reactions.

Initially, this kinetics study was performed with a highly reactive monomer **12** containing a terminal alkyne. Under a constant concentration of catalyst **A**, a 2-fold increase in the monomer concentration resulted in a doubling of the reaction rate, indicating that the reaction was first order in monomer **12** (Table 6, entries 1 and 2). This result suggested that the rate-

Table 6. Kinetics Study of Tandem RO/RCM Monomers



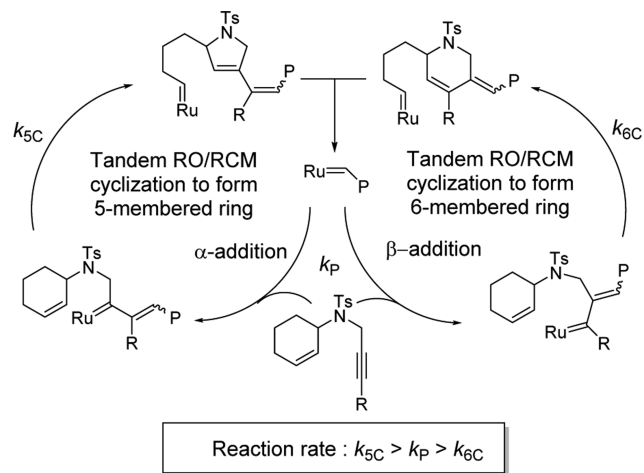
entry	monomer	[monomer]	[A]	rate ^a (M/s)
1 ^b	12	0.02 M	0.13 mM	8.90 × 10 ⁻⁴
2 ^b	12	0.01 M	0.13 mM	4.85 × 10 ⁻⁴
3	11e	0.03 M	0.2 mM	1.37 × 10 ⁻⁵
4	11e	0.02 M	0.2 mM	1.57 × 10 ⁻⁵
5	11e	0.01 M	0.2 mM	1.36 × 10 ⁻⁵
6	10	0.02 M	0.4 mM	8.40 × 10 ⁻⁵
7	10	0.01 M	0.4 mM	4.04 × 10 ⁻⁵
8	8	0.02 M	0.4 mM	1.52 × 10 ⁻⁵
9	8	0.01 M	0.4 mM	1.76 × 10 ⁻⁵

^aInitial rates were measured (see SI for detail). ^bThe reaction temperature was -10 °C.

determining step was the intermolecular propagation step, as observed for typical living polymerization reactions, and that five-membered-ring cyclization was indeed fast. However, in the case of monomer **11e**, which contained an internal alkyne with a 4-CF₃-phenyl substituent, the kinetics study revealed that the reaction was zeroth order in monomer concentration (i.e., changing the monomer concentration did not change the reaction rate) (entries 3–5). This result suggested that the rate-determining step for the polymerization of **11e** was the intramolecular RO/RCM step. At this point, which cyclization step was the actual rate-determining step remained unclear because the two different cyclizations were possible for the internal alkyne.^{6f,j,m} We therefore performed a kinetics study on monomer **10**, which possesses an internal alkyne with a CF₃ substituent, but only underwent five-membered-ring cyclization, and confirmed the first-order relationship in the monomer concentration, unlike **11e** containing a similar electron-withdrawing substituent (entries 6 and 7). This result implies that the propagation step was the rate-determining step and that the five-membered-ring cyclization was still fast for monomer **10**. Interestingly, although the structure of monomer **8** containing a methyl group might seem similar to **10**, the reaction order was still zero in the monomer concentration of **8** just like **11e** (entries 8 and 9). In short, the presence of a six-membered-ring cyclization step after β -addition seemed to dictate the reaction order.

On the basis of the series of kinetics data, we drew several conclusions. The kinetics study suggested that the five-membered-ring cyclization (k_{5C}) after α -addition was the fastest step, which logically led us to believe that six-membered-ring cyclization (k_{6C}) from β -addition was, surprisingly, the slowest step, becoming the rate-determining step for monomers containing internal alkynes (Scheme 4). In fact, a

Scheme 4. Reaction Kinetics of Tandem RO/RCM Polymerization



similar observation in which cyclopolymerization via five-membered-ring cyclization was much faster than that of six-membered-ring cyclization was reported.^{6g} This conclusion also agreed with the interpretation of ρ values obtained from the Hammett plot, which suggested that the rate-determining step involved the olefin metathesis reactions from benzylidenes after β -addition (Figure 4a). These results are unusual because the rate-determining step of conventional chain-growth polymerization reactions is typically the propagation step. Notably, with this understanding of the mechanism, where the cyclization step could be the rate-determining step, our previous failures, new proposals, and new strategies all became logically consistent. In short, controlling the intramolecular tandem RO/RCM cyclization is the key for successful polymerization.

CONCLUSION

We extensively studied the reaction mechanism of tandem RO/RCM polymerization to enhance polymerization efficiency for various challenging monomers. The previous unsuccessful polymerization was because of relatively slow intramolecular RO/RCM that led to the acceleration of competing side reactions such as intermolecular CM reactions. To this end, two strategies successfully solved this problem and greatly enhanced polymerization reactivity. First, we modified the monomer structures to accelerate the cyclization by enhancing the Thorpe–Ingold effect; this strategy also allowed living polymerization. Furthermore, the synthesis of dendronized polymers containing as large as third-generation dendrons was possible, and the resulting single polymer chain was visualized via AFM. The second strategy was to reduce the reaction concentration to favor the intramolecular RO/RCM step over competing side reactions. The monomer scope was then further expanded to those containing internal alkynes, and polymerization of these monomers was more challenging because the selectivity issue between α - and β -addition resulted in the

formation of more complex polymer microstructures comprising five- and six-membered-ring units. Nonetheless, polymerization of internal-alkyne-containing monomers was successful under dilute conditions, and their regioselectivity was governed by steric and electronic effects of the substituents. Lastly, the polymerization kinetics study and Hammett-plot analysis revealed the unique kinetics of tandem RO/RCM polymerization. As expected, the rate-determining step of the reactive monomers was the intermolecular propagation step. However, for challenging monomers containing internal alkynes, the intramolecular six-membered-ring cyclization step was the rate-determining step. This observation agrees well with all the data we obtained and validates our strategies. In conclusion, studying the mechanism in detail not only provided deep insights into the polymerization pathway but also provided clues to greatly improve the polymerization efficiency and broaden the monomer scope.

ASSOCIATED CONTENT

Supporting Information

The Supporting Information is available free of charge on the ACS Publications website at DOI: 10.1021/jacs.5b12223.

Experimental details, synthesis characterization data (¹H and ¹³C NMR, MS, SEC traces, etc.), and spectra of the compounds (PDF)

AUTHOR INFORMATION

Corresponding Author

*tlc@snu.ac.kr

Notes

The authors declare no competing financial interest.

ACKNOWLEDGMENTS

This paper is dedicated to Prof. Se Won Suh on his lifelong achievements in research and education at SNU and his retirement. We are grateful for the financial support from the Basic Science Research Program, and the Nano-Material Technology Development Program through the National Research Foundation of Korea. We also thank NCIRF at SNU for supporting GC-MS and ¹³C NMR experiments.

REFERENCES

- (1) (a) Grubbs, R. H.; Chang, S. *Tetrahedron* **1998**, *54*, 4413. (b) Fürstner, A. *Angew. Chem., Int. Ed.* **2000**, *39*, 3013. (c) Grubbs, R. H. *Handbook of Metathesis*, Vols. 1, 2; Wiley-VCH: Weinheim, 2003. (d) Grubbs, R. H. *Tetrahedron* **2004**, *60*, 7117.
- (2) (a) Schwab, P.; France, M. B.; Ziller, J. W.; Grubbs, R. H. *Angew. Chem., Int. Ed. Engl.* **1995**, *34*, 2039. (b) Schwab, P.; Grubbs, R. H.; Ziller, J. W. *J. Am. Chem. Soc.* **1996**, *118*, 100. (c) Scholl, M.; Ding, S.; Lee, C. W.; Grubbs, R. H. *Org. Lett.* **1999**, *1*, 953.
- (3) (a) Schrock, R. R.; Murdzek, J. S.; Bazan, G. C.; Robbins, J.; DiMare, M.; O'Regan, M. *J. Am. Chem. Soc.* **1990**, *112*, 3875. (b) Bazan, G. C.; Oskam, J. H.; Cho, H.-N.; Park, L. Y.; Schrock, R. R. *J. Am. Chem. Soc.* **1991**, *113*, 6899. (c) Feldman, J.; Schrock, R. R. *Prog. Inorg. Chem.* **1991**, *39*, 1.
- (4) For selected tandem metathesis reaction reports, see: (a) Kitamura, T.; Mori, M. *Org. Lett.* **2001**, *3*, 1161. (b) Ruckert, A.; Eisele, D.; Blechert, S. *Tetrahedron Lett.* **2001**, *42*, 5245. (c) Randl, S.; Lucas, N.; Connon, S. J.; Blechert, S. *Adv. Synth. Catal.* **2002**, *344*, 631. (d) Mori, M.; Kuzuba, Y.; Kitamura, T.; Sato, Y. *Org. Lett.* **2002**, *4*, 3855. (e) Banti, D.; North, M. *Adv. Synth. Catal.* **2002**, *344*, 694.
- (5) (a) Novak, B. M.; Grubbs, R. H. *J. Am. Chem. Soc.* **1988**, *110*, 960. (b) Schrock, R. R. *Acc. Chem. Res.* **1990**, *23*, 158. (c) Bielawski, C. W.; Grubbs, R. H. *Angew. Chem., Int. Ed.* **2000**, *39*, 2903.

- (6) For a review on olefin metathesis cyclopolymerization, see: (a) Choi, S.-K.; Gal, Y.-S.; Jin, S.-H.; Kim, H. K. *Chem. Rev.* **2000**, *100*, 1645. For examples of olefin metathesis cyclopolymerization, see: (b) Fox, H. H.; Wolf, M. O.; O'Dell, R.; Lin, B. L.; Schrock, R. R.; Wrighton, M. S. *J. Am. Chem. Soc.* **1994**, *116*, 2827. (c) Anders, U.; Nuyken, O.; Buchmeiser, M. R.; Wurst, K. *Angew. Chem., Int. Ed.* **2002**, *41*, 4044. (d) Anders, U.; Nuyken, O.; Buchmeiser, M. R.; Wurst, K. *Macromolecules* **2002**, *35*, 9029. (e) Mayershofer, M. G.; Nuyken, O.; Buchmeiser, M. R. *Macromolecules* **2006**, *39*, 3484. (f) Kang, E.-H.; Lee, I. S.; Choi, T.-L. *J. Am. Chem. Soc.* **2011**, *133*, 11904. (g) Lee, I. S.; Kang, E.-H.; Park, H.; Choi, T.-L. *Chem. Sci.* **2012**, *3*, 761. (h) Kim, J.; Kang, E.-H.; Choi, T.-L. *ACS Macro Lett.* **2012**, *1*, 1090. (i) Kang, E.-H.; Lee, I.-H.; Choi, T.-L. *ACS Macro Lett.* **2012**, *1*, 1098. (j) Park, H.; Lee, H.-K.; Choi, T.-L. *Polym. Chem.* **2013**, *4*, 4676. (k) Kang, E.-H.; Yu, S. Y.; Lee, I. S.; Park, S. E.; Choi, T.-L. *J. Am. Chem. Soc.* **2014**, *136*, 10508. (l) Song, J.-A.; Park, S.; Kim, T.-S.; Choi, T.-L. *ACS Macro Lett.* **2014**, *3*, 795. (m) Park, H.; Lee, H.-K.; Kang, E.-H.; Choi, T.-L. *J. Polym. Sci., Part A: Polym. Chem.* **2015**, *53*, 274. (n) Liu, W.; Liao, X.; Li, Y.; Zhao, Q.; Xie, M.; Sun, R. *Chem. Commun.* **2015**, *51*, 15320. (o) Song, W.; Han, H.; Wu, J.; Xie, M. *Polym. Chem.* **2015**, *6*, 1118.
- (7) (a) Wagener, K. B.; Boncella, J. M.; Nel, J. G. *Macromolecules* **1991**, *24*, 2649. (b) Patton, J. T.; Boncella, J. M.; Wagener, K. B. *Macromolecules* **1992**, *25*, 3862. (c) Brzezinska, K.; Wolfe, P. S.; Watson, M. D.; Wagener, K. B. *Macromol. Chem. Phys.* **1996**, *197*, 2065. (d) Mutlu, H.; de Espinosa, L. M.; Meier, M. A. R. *Chem. Soc. Rev.* **2011**, *40*, 1404.
- (8) For a few selective polymerizations using two or more metathesis reactions, see: (a) Choi, T.-L.; Rutenberg, I. M.; Grubbs, R. H. *Angew. Chem., Int. Ed.* **2002**, *41*, 3839. (b) Ding, L.; Xie, M.; Yang, D.; Song, C. *Macromolecules* **2010**, *43*, 10336. (c) Lee, H.-K.; Bang, K.-T.; Hess, A.; Grubbs, R. H.; Choi, T.-L. *J. Am. Chem. Soc.* **2015**, *137*, 9262. (d) Elling, B. R.; Xia, Y. *J. Am. Chem. Soc.* **2015**, *137*, 9922.
- (9) (a) Park, H.; Choi, T.-L. *J. Am. Chem. Soc.* **2012**, *134*, 7270. (b) Park, H.; Lee, H.-K.; Choi, T.-L. *J. Am. Chem. Soc.* **2013**, *135*, 10769.
- (10) Gutekunst, W. R.; Hawker, C. J. *J. Am. Chem. Soc.* **2015**, *137*, 8038.
- (11) (a) Kirby, A. J. *Adv. Phys. Org. Chem.* **1981**, *17*, 183. (b) Jung, M. E.; Gervay, J. *J. Am. Chem. Soc.* **1991**, *113*, 224.
- (12) Love, J. A.; Morgan, J. P.; Trnka, T. M.; Grubbs, R. H. *Angew. Chem., Int. Ed.* **2002**, *41*, 4035.
- (13) Eliel, E. L.; Wilne, S. H.; Mander, L. N. *Stereochemistry of Organic Compounds*; Wiley: New York, 1993; pp 696–697.
- (14) (a) Kim, K. O.; Choi, T.-L. *ACS Macro Lett.* **2012**, *1*, 445. (b) Kim, K. O.; Choi, T.-L. *Macromolecules* **2013**, *46*, 5905. (c) Kim, K. O.; Shin, S.; Kim, J.; Choi, T.-L. *Macromolecules* **2014**, *47*, 1351.
- (15) (a) Ihre, H.; Hult, A. *Macromolecules* **1998**, *31*, 4061. (b) Ihre, H.; De Jesús, O. L.; Ren, G.; Fréchet, J. M. J. *J. Am. Chem. Soc.* **2001**, *123*, 5908.
- (16) Stragies, R.; Voigtmann, U.; Blechert, S. *Tetrahedron Lett.* **2000**, *41*, 5465.
- (17) Adlhart, C.; Hinderling, C.; Baumann, H.; Chen, P. *J. Am. Chem. Soc.* **2000**, *122*, 8204.